Collisions between vector and scalar spatial solitons in Kerr media

M. Delqué, G. Fanjoux, T. Sylvestre

Collision between scalar and vector spatial solitons in Kerr media

Michaël Delqué · Gil Fanjoux · Thibaut Sylvestre

Abstract Experimental observation and numerical results concerning collisions between scalar and vector spatial solitons in a Kerr planar waveguide are presented. It is shown that this configuration allows for the full control of spatial and polarization dynamics of the interacting vector solitons. On the one hand, the ability to achieve polarization control of a single-hump vector soliton is demonstrated. On the other hand, the effect of collision on the spatial symmetry-breaking dynamics of multimode vector solitons is investigated.

Keywords Kerr effect · Soliton collision · Vector soliton

1 Introduction

Self-guided light beams result from the balance between linear diffractive and self-focusing effects induced in a nonlinear medium (Kivshar and Agrawal 2003). They have raised a lot of interest because of their ability to not only guide themselves but also other beams, while being fully configurable (Kivshar and Stegeman 2002). In view of potential applications, polarization vector solitons seem of particular interest because they can provide a wide variety of spatial and polarization dynamics (Gregori and Wabnitz 1986; Christodoulides and Joseph 1988; Tratnik and Sipe 1988; Islam et al. 1990; Silberberg and Barad 1995; Soto-Crespo et al. 1995). In particular, the spatial symmetry-breaking of multimode vector solitons in Kerr media spontaneously generates a waveguiding structure merging several channels to one (Silberberg and Barad 1995; Haelterman and Sheppard 1994a; Kockaert and Haelterman 1999). A widely considered way for applying solitons to future all-optical information technologies is using collisions between them. The spatial structure of soliton collision naturally explains the interest they raised and recent works have demonstrated some of their important features (Cao and Meyerhofer 1994; Kang et al. 1996; Anastassiou et al. 2001). They indeed

M. Delqué (✉) · G. Fanjoux · T. Sylvestre
Département d'Optique P.M. Duffieux, Institut FEMTO-ST, Université de Franche-Comté, CNRS UMR 6174, 25030 Besançon, France
e-mail: michael.delque@univ-fcomte.fr

offer the ability to couple, cross, reflect, deflect or merge information channels. Many spatial dynamics can be easily achieved by tuning the phase relation or the angle between solitons in scalar propagation (Snyder et al. 1995). Using the vector nature of spatial solitons opens the way for new opportunities. For instance, the collision between orthogonally polarized solitons induces inelastic interactions and complex energy exchanges between polarization components (Cao and Meyerhofer 1994) even if the solitons are initially single component. The spatial dynamics of these soliton collisions can also be very complex, including multiple reflections and trapping (Tan and Yang 2001; Schauer et al. 2004; Goodman and Haberman 2005). A few experimental results confirm these numerical and analytical expectations showing soliton trapping and dragging (Kang et al. 1996).

An even more complex way for colliding solitons is to use collisions between vector solitons. Such an interaction has been investigated in the well-known Manakov configuration and is in essence inelastic (Radhakrishnan et al. 1997). This feature can be applied to highly efficient polarization conversion (Radhakrishnan et al. 2004; Tchofo Dinda et al. 2007). These phenomena have been observed experimentally and applied to information transfer through energy switching between polarization components (Anastassiou et al. 1999; Anastassiou et al. 2001). In this paper, we present experimental and numerical results showing two collisions of spatial solitons in a vector configuration. In particular, we report on vector and scalar spatial soliton interaction involving different frequencies, polarizations or even modes at the same time. This is, to our knowledge, the first demonstration of the spatial and polarization dynamics that can be reached by mixing vector phenomena and soliton collision in Kerr media. In the first part of this paper, we introduce the theoretical and numerical model we use to describe the vector soliton collisions of light beams. In the two following parts, we present two experimental realizations on vector soliton collisions involving a scalar infrared and a multi-component vector green soliton. We first demonstrate the ability of such vector collisions to induce efficient polarization change of an initially circularly-polarized soliton. The second experiment is devoted to the study of the random symmetry-breaking of a multimode vector soliton induced by collision. Our results show that collision between vector and scalar solitons gives rise to new spatial or polarization dynamics that could be useful for realizing various all-optical switching functionalities.

2 Theoretical and numerical analysis

2.1 Vector propagation

Assuming a lossless and dispersionless nonlinear medium, monochromatic vector propagation in a single mode planar Kerr waveguide can be modeled by the usual system of 1+1D coupled nonlinear Schrödinger equations (NLSE) that reads (Chen et al. 1995):

$$\frac{\partial E_x}{\partial z} = \frac{\mathrm{i}}{2k_x}\frac{\partial^2 E_x}{\partial x^2} + \mathrm{i}\gamma\left\{\left[|E_x|^2 + (1-B)\left|E_y\right|^2\right]E_x + BE_y^2E_x^\star e^{2i\Delta kz}\right\} \tag{1a}$$

$$\frac{\partial E_y}{\partial z} = \frac{\mathrm{i}}{2k_y}\frac{\partial^2 E_y}{\partial x^2} + \mathrm{i}\gamma\left\{\left[\left|E_y\right|^2 + (1-B)\left|E_x\right|^2\right]E_y + BE_x^2E_y^\star e^{-2i\Delta kz}\right\} \tag{1b}$$

where z is the spatial coordinate along the longitudinal propagation direction and x is the spatial coordinate along the free unguided transverse direction of the waveguide. E_x, E_y are the transverse electric (TE) and magnetic (TM) orthogonal linearly polarized components of the electric field, respectively, while k_x and k_y are the wave vectors and $\Delta k = k_y - k_x$ is the

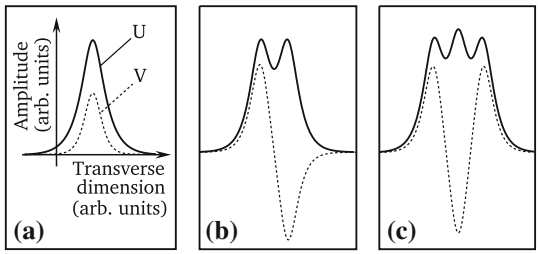

Fig. 1 Examples of numerical stationary solutions of Eq. 2. (**a**) Elliptically-polarized fundamental vector soliton, (**b**, **c**) higher-order multimode vector solitons

wave vector mismatch due to the intrinsic linear birefringence. $\gamma = 2\pi n_2/\lambda_0$ is the nonlinear coefficient with $n_2 = 3.5 \times 10^{-18}\mathrm{m^2W^{-1}}$ the nonlinear refractive index in CS_2 (see, e.g., Cambournac et al. 2002a) and $\lambda_0 = 532$ nm the wavelength in vacuum. $B = \chi_{xyyx}/\chi_{xxxx}$ represents the polarization susceptibility ratio. As the Kerr nonlinearity of CS_2 mainly relies on the molecular reorientation effect in the sub-nanosecond regime, $B = 3/4$ (Boyd 1992). Terms on the right hand side of Eq. 1 stand for diffraction, self-phase modulation (SPM), cross-phase modulation (XPM), and degenerate four-wave mixing (so-called FWM term), respectively. FWM is a coherent coupling process which can lead to strong energy exchange between E_x and E_y depending on the magnitude of Δk. In isotropic or low-birefringence media for which $\Delta k \simeq 0$, the energy transfer can be very efficient, thus leading to nonlinear effects such as polarization instability (Winful 1985; Wang et al. 1998), whereas in highly birefringent media, no efficient energy exchange occurs.

In isotropic media, $k_x = k_y = k$ and Eq. 1 can be rewritten in a more convenient way in the basis of circular polarizations as:

$$\frac{\partial U}{\partial z} = \frac{\mathrm{i}}{2k}\frac{\partial^2 U}{\partial x^2} + \mathrm{i}\gamma\left[(1-B)\,|U|^2 + (1+B)\,|V|^2\right]U \tag{2a}$$

$$\frac{\partial V}{\partial z} = \frac{\mathrm{i}}{2k}\frac{\partial^2 V}{\partial x^2} + \mathrm{i}\gamma\left[(1-B)\,|V|^2 + (1+B)\,|U|^2\right]V, \tag{2b}$$

where $U, V = \left(E_x \pm \mathrm{i}E_y\right)/\sqrt{2}$ are the left-handed and the right-handed circularly polarized components of the electric field, respectively. The family of vector solitons in isotropic Kerr media can be easily described using this basis (Haelterman and Sheppard 1994a; Haelterman et al. 1993) because of the incoherent coupling between U and V (see Eq. 2). The phase difference between U and V has no influence on the existence of theses bound states. It corresponds to different values of the polarization angle in the cycle of polarization rotation of these vector solitons (Haelterman and Sheppard 1994b; Delqué et al. 2007).

Figure 1(a) depicts the first member of the family, called elliptically polarized fundamental soliton (Haelterman and Sheppard 1994b), which was recently observed (Delqué et al. 2005a, 2007). It is the only stable member of the family. Higher-order vector solitons as those represented in Fig. 1(b, c) are unstable and give rise to spatial left–right symmetry breaking instability that was also recently evidenced (Cambournac et al. 2002b; Delqué et al. 2005b). The polarization and spatial behavior of these solitons make them particularly interesting for all-optical signal processing systems. We will see in the following that collisions makes these dynamics even more useful in such systems.

2.2 Equations of the collision

In this paper, we focus on the study of collisions between a scalar soliton and a multicomponent vector soliton. The aim of our study is to observe the inelastic collision features

previously described for single-component solitons (Cao and Meyerhofer 1994). We also would like to know how these collisions will alter the vector properties of the soliton, as it has been suggested for the case of Manakov soliton (Radhakrishnan et al. 2004; Tchofo Dinda et al. 2007).

More precisely, we experimentally study two types of collisions between a scalar infrared soliton (1,064 nm) and a vector green soliton (532 nm) in a isotropic Kerr planar waveguide. Using two different wavelengths with large frequency shift for soliton ensures an incoherent coupling. Moreover, from an experimental point of view, it is more convenient to independently analyze the two solitons. The infrared soliton will always be single component (in the E_x, E_y basis) and we will see that the collision with a vector soliton will not modify the state of polarization on the infrared beam. Instead, the polarization and spatial dynamics induced by collision will only be noticeable on the green beam.

To numerically account for these multicomponent and multicolor interactions together, we use the model described in (Tran et al. 1994). Because the wavelengths of the colliding fields are quite different, the coherent terms containing these two fields can be neglected contrary to polarization coherent ones (FWM in Eq. 1). The only effective multicolor coupling terms are incoherent cross-phase modulation ones. In our case, the cross-phase modulation coefficient between different frequencies equals 2 for linearly-polarized components and -1 for orthogonally-polarized components. This is relevant of re-orientational molecular nonlinearity, as in CS_2. Thus we define the multicolor XPM_m terms: $XPM_{m\parallel}$ and $XPM_{m\perp}$. The NLS describing the evolution of one component of the green vector soliton writes:

$$\frac{\partial E_j}{\partial z} - \frac{i}{2k_0}\frac{\partial^2 E_j}{\partial x^2} - ic_{NL}^E\left\{\left[\underbrace{|E_j|^2}_{\text{SPM}} + \underbrace{(1-B)|E_l|^2}_{\text{XPM}}\right]E_j + \underbrace{BE_l^2E_j^*}_{\text{FWM}}\right\} - ic_{NL}^E\left(\underbrace{2|F_j|^2}_{\text{XPM}_{m\parallel}}\underbrace{-|F_l|^2}_{\text{XPM}_{m\perp}}\right)E_j = 0$$

where $j = x, y$ and $l = y, x$. F_x, F_y stand for the infrared components. To make the system equation complete, the same equation must be written for F_j ($j = x, y$) by exchanging E and F in Eq. 3. As we said previously, $F_y = 0$ is an input condition.

3 Experiments

3.1 Collision between single-hump solitons

In a first experiment, the linearly-polarized infrared soliton enters into collision in the nonlinear waveguide with a circularly-polarized green one and we analyze at the waveguide's output the induced polarization change on both beams. As previously said, circular basis is more convenient to describe vector solitons in an isotropic Kerr medium. This experiment aims at studying the result of such a collision on a single component in this basis.

The experiment, schematically sketched in Fig. 2, is performed in a 7 cm-long CS_2 liquid planar slab waveguide. The step-index waveguide is made of a 15 μm-thick CS_2 layer sandwiched between two SK5 glass plates, whose index difference is $\Delta n = 0.04$ (Cambournac et al. 2002b). A beat length of $L = 1.8$m much longer than the waveguide length was measured, which ensures a quasi isotropic regime. As a pump laser, we used a compact passively Q-switched powerchip Nd:YAG laser emitting 450 ps Gaussian pulses at a repetition rate of 1 kHz and at a wavelength of 1,064 nm (mean power is 90 mW). The laser beam is frequency

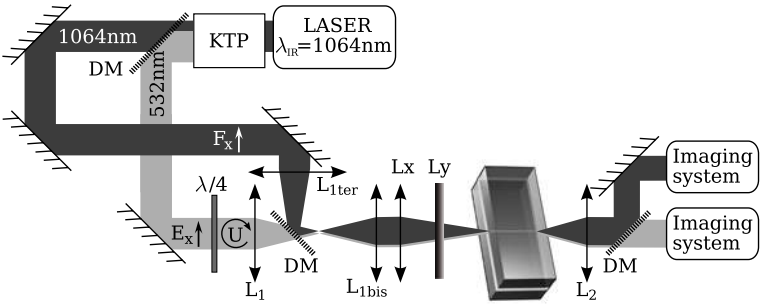

Fig. 2 Experimental setup

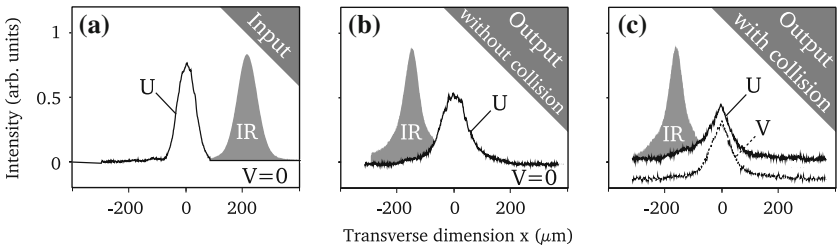

Fig. 3 Experimental profiles. (**a**) input, (**b**) output when the beams are not injected simultaneously and (**c**) output when the collision occurs

doubled in a KTP (Potassium Titanyl Phosphate) crystal. Each wavelength component is separated thanks to a dichroic mirror (DM). The green field is circularly-polarized by the use of a quarter-wave plate.The fundamental (1,064 nm) and second-harmonic (532 nm) radiations are shaped by using two couples of lenses (L_{1bis}, L_{1ter}) and (L_1, L_{1bis}), respectively. They are then recombined by a second dichroic mirror and launched in the planar waveguide by the (L_x, L_y) cylindrical lenses. At the output of the waveguide, once again they are divided, analyzed in polarization and imaged on CCD cameras.

The infrared soliton is polarized along the free transverse x direction of the waveguide and crosses the straight route of the green circularly polarized beam. Input spatial profiles are shown in Fig. 3(a). We see the infrared and the green input gaussian profiles separated by a distance of 220μ m. Figure 3(b) shows the output profiles when beams are injected independently, i.e., when no collision occurs. We clearly see the generation of the sech-shaped infrared soliton through the measure of the beam widths: $\Delta x_{in}^{IR} = 80\mu$ m and $\Delta x_{out}^{IR} = 75\mu$ m. In comparison with its input transverse position, it has moved apart from the green beam towards $x < 0$ by almost -400μ m. This corresponds for 7-cm propagation to a collision angle of $\sim 1.8 \times 10^{-3}\pi$ rad, which is in the range of angles studied in Kang et al. (1995). Figure 3(b) also shows that the green beam does not reach exact soliton propagation. Indeed $\Delta x_{in} = 75\mu$ m and $\Delta x_{out} = 100\mu$ m. However, purely linear propagation would result in $\Delta x_{out} \approx 140\mu$ m, thus we are in between soliton and linear propagation. As expected from isotropic condition, Fig. 3(b) shows that its state of polarization remains circular at the output of the waveguide since no energy appears in the V component.

Figure 3(c) depicts the experimental output profiles when the collision enters into play. What we first see is that the infrared soliton has not been altered by this collision, neither in its spatial nor in its polarization characteristics. On the other hand, the polarization of the

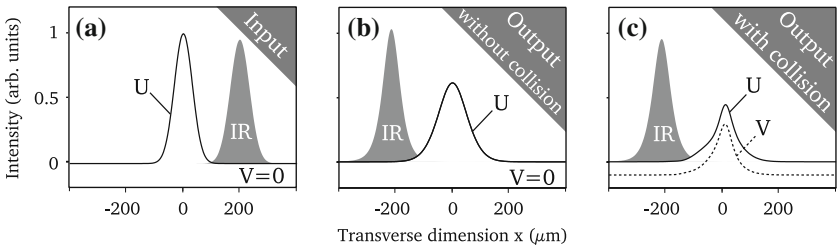

Fig. 4 Numerical profiles. (**a**) input, (**b**) output when the beams are not injected simultaneously and (**c**) output when the collision occurs

green beam is substantially modified after collision leading to the generation of an opposite right-handed circular polarization component V. Figure 3(c) shows that the intensity of this component is close to the U one (Note that we plot the V intensity profile with an offset to clearly distinguish the two components). Moreover, the width of the total green beam becomes narrower than the previous case ($\Delta x_{out} = 75\mu$ m) although the input power is the same as in Fig. 3(b). This can be explained by the fact that the green soliton undergoes self-focusing after collision owing to the strong state of polarization change.

This collision-induced polarization change is confirmed by the numerical simulations in Fig. 4 that shows the input and output of both the infrared soliton (gray scale) and the green soliton (solid and dashed lines). The agreement with experimental profiles of Fig. 3 is very good. The physical explanation of this effect is quite simple in terms of nonlinearly-induced birefringence. Actually, the infrared soliton induces through XPM_m a strong nonlinear birefringence which is seen by the green soliton. Thus the green soliton does not propagate in an isotropic medium anymore where the collision occurs, and its polarization changes resulting in the appearance of the V component. This means that its polarization is no longer circular, resulting in a more efficient self-focusing and a smaller beam width at the waveguide's output. The green soliton will in turn induce a nonlinear birefringence leading to a polarization change of the infrared one. But the experimental and numerical results of Figs. 3 and 4 do not show this phenomena. Indeed, at the beginning of the collision, the green beam is circularly polarized and induces no birefringence. Its polarization has efficiently changed only at the very end of the collision, that's why the infrared soliton does not noticeably suffer the induced birefringence. To verify this hypothesis, we have performed additional numerical simulations with longer interaction lengths (i.e., smaller angles) that demonstrate that the infrared polarization can also be modified. The most interesting feature of this experiment relies on the fact that the green beam remains self-guided and spatially stable while suffering polarization change. Given the diversity of the collision parameters, namely, relative powers of the solitons, collision angle, relative polarization, we can expect a wide variety of output polarization states of the green beam.

3.2 Collision between scalar and higher-order vector solitons

Another interesting application of vector soliton collision is to induce the symmetry-breaking of multimode vector solitons as those shown in Fig. 1(b) and (c) (Silberberg and Barad 1995; Cambournac et al. 2002b). As previously demonstrated for the case of the bimodal vector soliton (Kockaert and Haelterman 1999), this instability results from the exponential amplification of pertubative modes, leading to an efficient left–right energy switching between the two modes of the soliton. Since the instability can start from a very small perturbation,

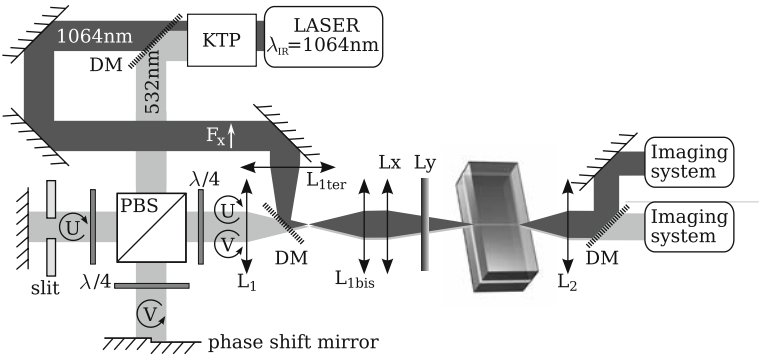

Fig. 5 Experimental setup

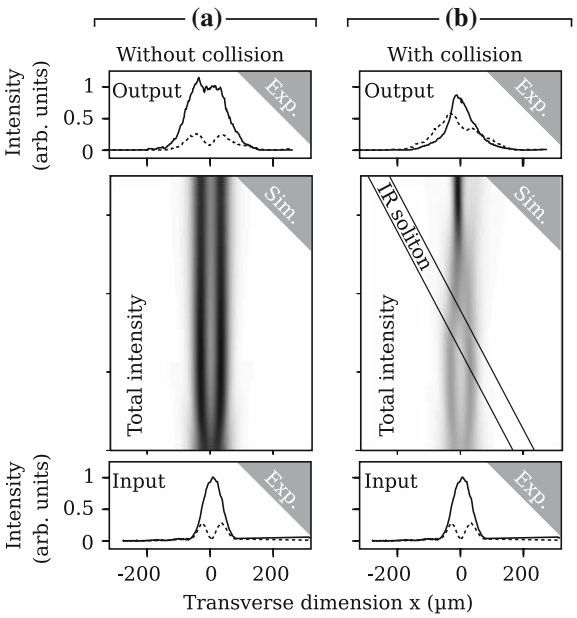

Fig. 6 Input and output experimental profiles and corresponding longitudinal simulation of: (**a**) the propagation of a green multimode vector soliton; (**b**) the collision of the same multimode vector soliton and an infrared soliton. Profiles depict the U (continuous line) and V (dashed line) components

e.g., quantum noise, it is difficult to control it, and this therefore leads to a random left–right output (Lantz et al. 2004). The aim of the present work is to induce through collision the symmetry-breaking dynamics before such random dynamics develop. Thus we can expect a full control of the vector soliton symmetry breaking in view of potential applications to all-optical N→1 junctions (Cambournac et al. 2002b; Delqué et al. 2005b).

The experimental setup is depicted in Fig. 5. It is very similar to the previous one, in particular concerning the infrared beam. As regards the green one, we insert in the setup a Michelson-type interferometer to independently generate the symmetric U and antisymmetric V components of the bimodal vector soliton. In the first arm, we only use a slit in order to tune the width of U. In the other one, a phase-shift mirror ensures that the sides of V are π-out of phase. The end of the setup is the same as in Fig. 2.

Experimental profiles and corresponding numerical simulations are summarized in Fig. 6. In this figure we compare the stable propagation of the multimode vector soliton alone

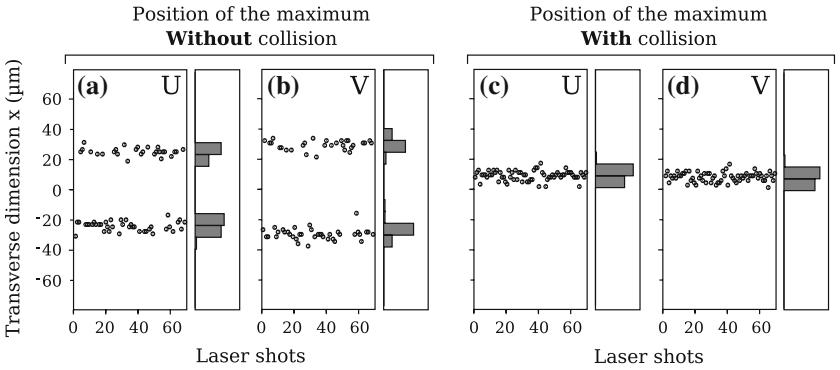

Fig. 7 Numerical results. Position of the intensity maximum after 7 cm propagation for both the U and V components: (**a**, **b**) when the multimode vector soliton propagates alone and (**c**, **d**) when the collision with the linearly polarized infrared soliton occurs

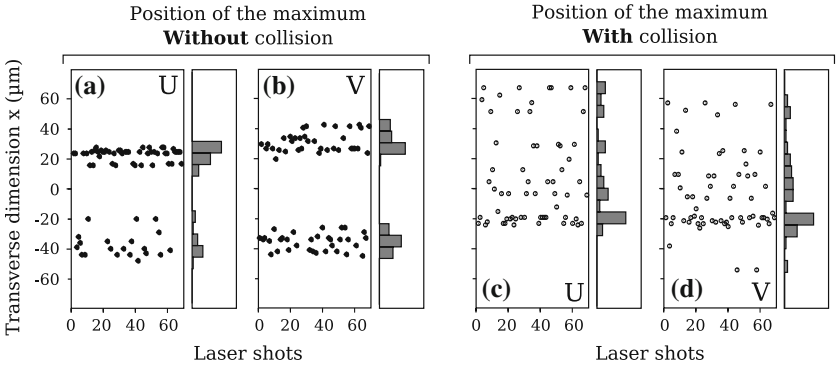

Fig. 8 Experimental results. Position of the intensity maximum after 7 cm propagation for both the U and V components: (**a**, **b**) when the multimode vector soliton propagates alone and (**c**, **d**) when the collision with the linearly polarized infrared soliton occurs

in Fig. 6(a) with the same one perturbed by the collision with the scalar infrared soliton. Figure 6(b) shows that the soliton collision induces the symmetry-breaking of the multimode vector soliton, as expected. Once again this can be physically understood on the basis of the nonlinear birefringence induced by the infrared soliton. We must stress that the data plotted on this figure are averaged over tens of pulses. As the propagation is unstable due to symmetry-breaking, these results only have a statistical meaning and do not correspond to one-shot output profiles. When the green vector soliton propagates alone, the random nature of its breaking dynamics results in symmetric output statistics, as shown in top of Fig. 6(a). This means that as many left and right symmetry-breaking events are observed, along with stable soliton bound-state events (Cambournac et al. 2002b). When the collision occurs, however, the statistics clearly changes. We also observe in the top of Fig. 6(b) energy exchanges between U and V as in the previous section. To get better insight into the breaking dynamics, we performed shot-to-shot analysis.

Numerical results of such an analysis are described in Fig. 7. We ran as many numerical simulations (70) as experimental corresponding data recorded and represented in Fig. 8. Every single simulation includes a different small input random amplitude noise. In Fig. 7 we

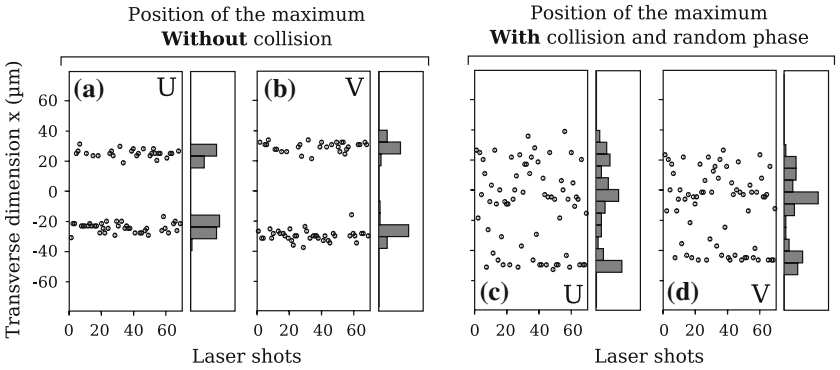

Fig. 9 Results of simulations taking into account the random phase relation between U and V green components. Position of the intensity maximum after 7 cm propagation for both components: (**a**, **b**) when the multimode vector soliton propagates alone and (**c**, **d**) when the collision with the linearly polarized infrared soliton occurs

show the position of the maxima of both green components, with and without the collision in order to identify on which side the energy switches. Figure 7(a, b) show the positions of these maxima without collision. These figures show the random left–right spatial dynamics corresponding to the spontaneous symmetry-breaking instability.

Figure 7(c, d) represent the collision in the same conditions as in Fig. 7(a, b). We now see that the collision suppresses the random nature of the symmetry-breaking. The vector soliton bound-states always follows the same breaking dynamics towards $x > 0$.

Figure 8 illustrates the corresponding experimental observations. We show in Fig. 8(a, b) the left–right random symmetry-breaking dynamics of the unperturbed multimode vector soliton. In Fig. 8(c,d), we cannot observe the same results as in the simulations of Fig. 7(c, d). We see that the breaking statistics has dramatically changed, but we could not erase the random behavior. Indeed a preferred direction of switching can be identified around $x = -20\mu$ m but the dispersion of the values is as large as in the collisionless configuration.

This can be easily understood by considering the random phase difference of the vector soliton U and V components. Let us recall that the interaction between the infrared and the green soliton are assumed incoherent thus their relative phase has no influence. But, as the collision acts through $\mathrm{XPM}_{m\parallel}$ and $\mathrm{XPM}_{m\perp}$ ($\mathrm{XPM}_{m\parallel} \neq \mathrm{XPM}_{m\perp}$), the result depends on the exact polarization state of the green beam. This state strongly depends on the relative phase between U and V which defines its orientation angle (Delqué et al. 2007). Unfortunately, our experimental conditions did not allow for the achievement of the full control of the relative phase difference between the two components U and V of the vector soliton. As a result, we obtain random shot-to-shot polarization angle, inducing random collision results, as observed in Fig. 8(c, d). Note that this random polarization orientation has no effect on the green soliton generation, as it corresponds to different steps in the polarization rotation cycle of the same soliton, but it prevents us from suppressing the random behavior.

This explanation has been confirmed by additional simulations as in Fig. 7 but taking into account the random phase relation between U and V. The results of these simulations are depicted in Fig. 9. We observe that in such configuration, the collision does not prevent from random behavior and that the dispersion of the output positions is as large as in the collisionless case. Finally, these results show that a full control of symmetry breaking instability can be achieved by phase locking the two components of the vector soliton.

4 Conclusion

In this paper, we reported two examples of vector soliton collision in isotropic Kerr media. We first demonstrated the ability of such collisions to achieve all-optical polarization control of a self-guided beam. This ability was explained as resulting from the nonlinearly-induced birefringence between the solitons. Then we investigated the control of the symmetry breaking instability of multimode vector solitons by collision. We achieved experimentally the modification of the symmetry-breaking dynamics of theses solitons but not the total suppression of the random nature, owing to the random phase difference between the components of the vector soliton. Finally, these two examples showed that the collisions between vector and scalar solitons give rise to new spatial or polarization dynamics that could be useful in various all-optical switching techniques.

References

Anastassiou, C., Segev, M., Steiglitz, K., Giordmaine, J.A., Mitchell, M., Shih, M.-F., Lan, S., Martin, J.: Energy-exchange interactions between colliding vector solitons. Phys. Rev. Lett. **83**, 2332–2335 (1999)

Anastassiou, C., Fleisher, J.W., Carmon, T., Segev, M., Steiglitz, K.: Information tranfer vis cascaded collisions of vector solitons. Opt. Lett. **26**, 1498–1500 (2001)

Boyd, R.W.: Nonlinear Optics. Academic Press, San Diego (1992)

Cambournac, C., Maillotte, H., Lantz, E., Dudley, J.M., Chauvet, M.: Spatiotemporal behavior of periodic arrays of spatial solitons in a planar waveguide with relaxing Kerr nonlinearity. J. Opt. Soc. Am. B **19**, 574–585 (2002a)

Cambournac, C., Sylvestre, T., Maillotte, H., Vanderlinden, B., Kockaert, P., Emplit, P., Haelterman, M.: Symmetry-breaking instability of multimode vector solitons. Phys. Rev. Lett. **89**, 083901 (2002b)

Cao, X.D., Meyerhofer, D.: All-optical switching by means of collisions of spatial vector solitons. Opt. Lett. **19**, 1711–1713 (1994)

Chen, J.T., Liu, Q.D., Ho, P.P., Alfano, R.R.: Comparison of nonlinear effects of linearly and circularly polarized picosecond pulses propagationg in optical fibers. J. Opt. Soc. Am. B **12**, 907–912 (1995)

Christodoulides, D.N., Joseph, R.I.: Vector solitons in birefringent nonlinear dispersive media. Opt. Lett. **13**, 53–55 (1988)

Delqué, M., Sylvestre, T., Maillotte, H., Cambournac, C., Kockaert, P., Haelterman, M.: Experimental observation of the elliptically polarized fundamental vector soliton of isotropic Kerr media. Opt. Lett. **30**, 3383–3385 (2005a)

Delqué, M., Chauvet, M., Maillotte, H., Sylvestre, T.: Numerical and experimental investigations of vector soliton bound-states in a Kerr planar waveguide. Opt. Commun. **249**, 285–291 (2005b)

Delqué, M., Fanjoux, G., Sylvestre, T.: Polarization dynamics of the fundamental vector soliton of isotropic Kerr media. Phys. Rev. E **75**, 016611 (2007)

Goodman, R.H., Haberman, R.: Vector-soliton collision dynamics in nonlinear optical fibers. Phys. Rev. E **71**, 056605 (2005)

Gregori, G., Wabnitz, S.: New exact solutions and bifurcations in the spatial distribution of polarization in third-order nonlinear optical interactions. Phys. Rev. Lett. **56**, 600–603 (1986)

Haelterman, M., Sheppard, A.P.: Bifurcation phenomena and multiple soliton-bound states in isotropic Kerr media. Phys. Rev. E **49**, 3376–3381 (1994a)

Haelterman, M., Sheppard, A.P.: The elliptically polarized fundamental vector soliton of isotropic Kerr Media. Phys. Lett. A **194**, 191–196 (1994b)

Haelterman, M., Sheppard, A.P., Snyder, A.W.: Bound-vector solitary waves in isotropic nonlinear dispersive media. Opt. Lett. **18**, 1406–1408 (1993)

Islam, M.N., Soccolich, C.E., Gordon, J.P.: Soliton intensity-dependent polarization rotation. Opt. Lett. **15**, 21–23 (1990)

Kang, J.U., Stegeman, G.I., Aitchison, J.S.: Weak-beam trapping by bright spatial solitons in AlGaAs planar waveguides. Opt. Lett. **20**, 2069–2071 (1995)

Kang, J.U., Stegeman, G.I., Aitchison, J.S., Akhmediev, N.N.: Observation of Manakov spatial solitons in AlGaAs planar waveguides. Phys. Rev. Lett. **76**, 3699–3702 (1996)

Kivshar, Y.S., Agrawal, G.P.: Optical Solitons: from Fibers to Photonic Crystals. Academic Press, San Diego (2003)

Kivshar, Y.S., Stegeman, G.I.: Spatial Optical Solitons. Guiding Light for Future Technologies. Opt. Photon. News, **13**, 59–63 (2002)
Kockaert, P., Haelterman, M.: Stability and symmetry breaking of soliton bound states. J. Opt. Soc. Am. B **16**, 732–740 (1999)
Lantz, E., Sylvestre, T., Maillotte, H., Treps, N., Fabre, C.: Quantum fluctuations and correlations of spatial scalar or multimode vector solitons in Kerr media. J. Opt. B **6**, S295–S302 (2004)
Radhakrishnan, R., Lakshmanan, M., Hietarinta, J.: Inelastic collision and switching of coupled bright solitons in optical fibers. Phys. Rev. E **56**, 2213 (1997)
Radhakrishnan, R., Tchofo Dinda, P., Millot, G.: Efficient control of the energy exchange due to the Manakov vector-soliton collision. Phys. Rev. E **69**, 046607 (2004)
Schauer, A., Mel'nikov, I.V., Aitchison, J.S.: Collisions of orthogonally polarized spatial solitons in AlGaAs slab waveguides. J. Opt. Soc. Am. B **21**, 57–62 (2004)
Silberberg, Y., Barad, Y.: Rotating vector solitary waves in isotropic fibers. Opt. Lett. **20**, 246–248 (1995)
Snyder, A.W., Mitchell, D.J., Haelterman, M.: Parallel spatial solitons. Opt. Commun. **116**, 365–368 (1995)
Soto-Crespo, J.M., Akhmediev, N., Ankiewicz, A.: Soliton propagation in optical devices with two-component fields: a comparative study. J. Opt. Soc. Am. B **12**, 1100–1109 (1995)
Tan, Y., Yang, J.: Complexity and regularity of vector-soliton collisions. Phys. Rev. E **64**, 056616 (2001)
Tchofo Dinda, P., Radhakrishnan, R., Kanna, T.: Energy-exchange collision of the Manakov vector solitons under strong environmental perturbations. J. Opt. Soc. Am. B **24**, 592–605 (2007)
Tran, H.T., Sammut, R.A., Samir, W.: Multi-frequency spatial solitons in Kerr media. Opt. Commun. **113**, 292–304 (1994)
Tratnik, M.V., Sipe, J.E.: Bound solitary waves in a birefringent optical fiber. Phys. Rev. A **38**, 2011–2017 (1988)
Wang, D., Barillé, R., Rivoire, G.: Influence of soliton propagation on the beam-polarization dynamics in a planar waveguide. J. Opt. Soc. Am. B **15**, 2731–2737 (1998)
Winful, H.G.: Self-induced polarization changes in birefringent optical fibers. Appl. Phys. Lett. **47**, 213–215 (1985)